JOURNAL OF CHEMICAL & ENGINEERING DATA

Article

pubs.acs.org/jced

Vapor Pressure and Evaporation Coefficient of Silicon Monoxide over a Mixture of Silicon and Silica

Frank T. Ferguson*,[†] and Joseph A. Nuth, III[‡]

[†]Department of Chemistry, Catholic University, Washington, DC 20064, United States

[‡]NASA-Goddard Space Flight Center, Greenbelt, Maryland 20771, United States

ABSTRACT: The evaporation coefficient and equilibrium vapor pressure of silicon monoxide over a mixture of silicon and vitreous silica have been studied over the temperature range (1433 to 1608) K. The evaporation coefficient for this temperature range was (0.007 ± 0.002) and is approximately an order of magnitude lower than the evaporation coefficient over amorphous silicon monoxide powder and in general agreement with previous measurements of this quantity. The enthalpy of reaction at 298.15 K for this reaction was calculated via second and third law analyses as (355 ± 25) kJ·mol^{-1} and (363.6 ± 4.1) kJ·mol^{-1}, respectively. In comparison with previous work with the evaporation of amorphous silicon monoxide powder as well as other experimental measurements of the vapor pressure of silicon monoxide gas over mixtures of silicon and silica, these systems all tend to give similar equilibrium vapor pressures when the evaporation coefficient is correctly taken into account. This provides further evidence that amorphous silicon monoxide is an intimate mixture of small domains of silicon and silica and not strictly a true compound.

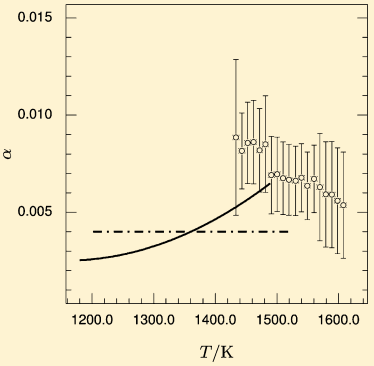

INTRODUCTION

The thermodynamics of the silicon−oxygen (Si−O) system are extremely important in understanding and improving the growth of silicon monoscrystals grown by the Czochralski (Cz) method for the semiconductor industry. In these systems the transport of oxygen in the silicon melt to the crystal growth interface plays an important role in the final properties of the resulting silicon wafers.[1] One of the challenges of growing larger crystals via the Czochralski process is the attack of the molten silicon on the silica glass crucible that occurs during the longer process times required for these larger crystals.[2,3] These pits form as small particles break off from the crucible and may be transported to the crystal interface, forming dislocations. Another potential problem is that the silicon monoxide (SiO) gas liberated during the crystal growth may condense above the melt, forming deposits that could potentially fall back into the melt and also contaminate the growing crystal.[3] Data on the silicon−silica system and the vapor pressure of SiO over such a mixture can be useful in modeling and optimizing Cz−Si growth.[4,5]

Another area in which the properties of the Si−O system are important is the modeling of grain formation in stellar outflows. One of the most abundant species in the outflows of oxygen-rich, asymptoptic giant branch (AGB) stars is believed to be silicon monoxide. Despite its relatively high abundance, previous models of these outflows seem to indicate that silicon monoxide would not appreciably nucleate until approximately 600 K, well below the observed formation of silicate grains above 1000 K in these oxygen-rich stars.[6] Therefore, other less abundant, but more refractory species were theorized to form a seed nucleus upon which silicon monoxide could later condense.

In a previous work, the vapor pressure and evaporation coefficient of silicon monoxide over amorphous silicon monoxide powder was measured.[7] These data coupled with previous measurements of SiO vapor pressure showed that the actual vapor pressure of SiO at approximately 1000 K and below was much lower than the expression that had been previously used in modeling SiO nucleation and growth,[8,9] thereby greatly increasing the possibility that SiO is the initial condensate in oxygen-rich, stellar outflows.[10]

In this earlier work, both the evaporation coefficient and the vapor pressure of $SiO_{(g)}$ over $SiO_{(am)}$ were measured. In this present study, these same quantities are measured for the following reaction:

$$1/2Si_{(cr)} + 1/2SiO_{2(vit)} \rightarrow SiO_{(g)} \quad (1)$$

In both the case of this silicon and silica reaction as well as the sublimation of amorphous silicon monoxide, the product is silicon monoxide gas. Brewer and Edwards reviewed the available thermodynamic and spectroscopic data on the silicon−oxygen system and concluded that the reaction given by eq 1 yields virtually pure silicon monoxide gas and that this gas is a monomer.[11] Later, this thermodynamic assessment was experimentally proven by Porter et al.[12] Using mass spectrometry, these authors were able to verify that the predominant species in the vapor over eq 1 was silicon

Received: July 7, 2011
Accepted: January 14, 2012
Published: February 2, 2012

monoxide gas, with Si_2O_2 being the next abundant species at a concentration approximately 4 orders of magnitude smaller.

For many years, there has been a controversy as to whether $SiO_{(am)}$ is a compound or simply an intimate, stoichiometric mixture of silicon (Si) and silica (SiO_2).[13] Recent works seem to confirm that $SiO_{(am)}$ is actually a mixture with very fine domains (~5 nm) of Si and SiO_2.[14,15] In studies of the vapor pressure of silicon monoxide gas, low evaporation coefficients have been noted for both systems. For example, the evaporation coefficient for $SiO_{(am)}$ has been measured as approximately 0.05 while the evaporation coefficient for $SiO_{(g)}$ over a mixture of Si and SiO_2 is typically an order of magnitude smaller. Such low evaporation coefficients were measured by Rocabois et al. for both systems.[16] Furthermore, these authors note that, within the experimental uncertainty for their system, both systems yielded the same vapor pressure for silicon monoxide gas when the evaporation coefficients were taken into account. In a previous work, both the evaporation coefficient and the vapor pressures for silicon monoxide gas over $SiO_{(am)}$ were in very good agreement with the results from Rocabois et al.[7] In this work, we report measured evaporation coefficients and equilibrium vapor pressures for silicon monoxide gas over a mixture of silicon and silica and compare these data with previous measurements.

EXPERIMENTAL APPARATUS AND PROCEDURE

The vapor pressure over the silicon−silica mixture is measured by monitoring the mass loss from a Knudsen effusion cell using a thermogravimetric balance. The thermogravimetric balance used in this work, a Thermo-Cahn 2171, is capable of reaching temperatures of 1973 K. The furnace tube of this balance is connected to mechanical and turbomolecular pumping system that maintains the pressure $<10^{-3}$ Pa in the sample area. The resulting mass loss from the sample cell is continuously recorded with a computer connected to the balance. During an experimental run, the sample cell is suspended on the sample side of the balance arm and centered within the furnace section of the reaction tube. This section is heated using six resistive heating elements. The temperature within the furnace is measured with a type-B thermocouple sheathed in an alumina tube and positioned approximately 0.5 cm below the bottom of the Knudsen cell.

The Knudsen cell used in this work is constructed from the closed-end sections of two different-sized, 99.8 % alumina tubes as shown in Figure 1. A smaller inner tube with a drilled orifice is cut and inverted in a close-fitting, larger tube. A window in the outer tube is cut, and the orifice of the inner tube is positioned in this this window. Although there is little clearance between the tubes, the tubes are also sealed at the top and the window areas with a zirconia-based adhesive (Resbond 904, Cotronics Corp.). All parts in the hot furnace zone area are made of 902 alumina with the exception of this zirconia adhesive, and in this case the minimum amount necessary to seal the cell is used.

Diamond-coated drill bits are used to produce the small effusion orifices in the alumina cells. Because of their small size, very high speed rotational rates are needed, and the bit must be fed at extremely slow feed rates. In this work a high speed air grinder (~85 000 rpm) was used, and it was fed using a computer controlled stage. This allowed the production of very clean orifices down to approximately 0.5 mm.

Before any experiments were performed, an equilmolar mixture of silicon powder (100 mesh, Alfa Products) and silicon dioxide (Mathey "Specpure" grade) was prepared and stored in a sealed container. Samples for all of the runs in this work were taken from this same container. For an experiment, alumina tubes were cut to construct a cell as shown in Figure 1, and an orifice was then drilled in the smaller tube. To measure the orifice diameter, the cell was placed under a microscope and measured with the aid of a traveling stage of micrometer accuracy.[7,17] After filling the cell with the Si/SiO_2 mixture, the cell was sealed with the zirconia cement and allowed to cure. After curing, the cell would be placed on the sample side of the balance within the furnace tube and evacuated for 24 h at room temperature. The sample was then heated to various temperatures, and the mass of the sample cell was continuously monitored, taking temperature and mass measurements twice per second.

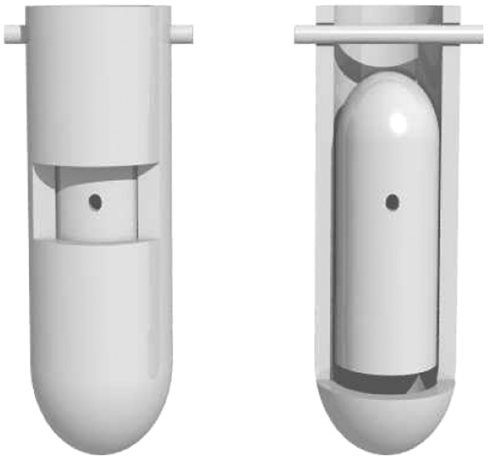

Figure 1. Alumina effusion cell constructed from two closed-end tubes.

In the same manner as was done for a previous study with silicon monoxide, after a run 2 min averages of the resulting large data set were taken for both the temperature and the mass data points. These data were then processed by a computer program to calculate the mass loss rates as a function of temperature. In this program, the temperature data were searched for regions where the temperature remained essentially constant. For these isothermal periods, the rates of mass loss were constructed from these 2 min averages. All of these values for an isothermal period were then averaged, and the standard deviation of this mean value was then used as an estimate of the uncertainty in this mass loss rate and used in the calculation of the vapor pressure.

VAPOR PRESSURE CALCULATION

The measured vapor pressure, P_m, is related to the mass loss rate, $\dot{m}$, via the Hertz−Knudsen equation:

$$P_m = \frac{\dot{m}}{W_B B}\sqrt{\frac{2\pi RT}{M_w}} \quad (2)$$

where B is the cross-sectional area of the effusion orifice, R is the gas constant, T is the temperature of the gas, and M_w is the molecular weight of the effusate. The term, W_B, is the Clausing correction factor for the cell orifice. If the cell wall thickness is knife-edge thin, this factor is 1.0. If, as is typical, the wall in the vicinity of the orifice has some finite thickness, this short "pipe" can cause an impedance to the transmission of molecules from the cell. This factor, W_B, accounts for this back-reflection of

dx.doi.org/10.1021/je200693d | J. Chem. Eng. Data 2012, 57, 721−728

some of the molecules and is based on the work of Clausing.[18] For arbitrary geometries, this factor must be computed from the Clausing integral equation. Berman developed a series expansion approximation to this equation for capillaries, and this formula has been used to calculate the Clausing factors for the cell.[19] For an effusion orifice of radius, a, and wall thickness ("pipe" length), l, the Clausing coefficient, W, is given by

$$W = Q_1 - Q_2 \tag{3}$$

where

$$Q_1 = 1 + (L^2/4) - (L/4)(L^2 + 4)^{1/2} \tag{4}$$

$$Q_2 = [(8 - L^2)(L^2 + 4)^{1/2} + L^3 - 16]^2 / [72{\cdot}L(L^2 + 4)^{1/2} - 288 \ln[L + (L^4 + 4)^{1/2}] + 288 \ln 2] \tag{5}$$

and

$$L = l/a \tag{6}$$

The accuracy of this equation has been verified by Monte Carlo simulations,[20] and this expression is reported to be better than 0.1 % for $0 \leq L \leq 5$, a range common to Knudsen effusion studies.[21]

As noted in the Introduction, silicon monoxide is expected to have a low evaporation coefficient. Whitman and Motzfeldt developed the following equation to account for such low evaporation coefficients in Knudsen cells:[22,23]

$$P_{eq} = \left[1 + f\left(\frac{1}{\alpha} + \frac{1}{W_A} - 2\right)\right] P_m \tag{7}$$

In this equation the impedance of the flow of molecules to the effusion orifice height is included in the term given by W_A, the Clausing factor for the cell. The term, P_{eq}, is the true, equilibrium vapor pressure, α, is the evaporation coefficient, and the term f is a factor related to the cell geometry and is given by

$$f = \frac{W_B B}{Ak} \tag{8}$$

where A is the cross-sectional area of the cell and k is the ratio of the effective evaporation surface area to the cell cross-sectional area. Therefore, the product Ak gives the actual evaporation surface area. In general, k is very difficult to accurately quantify and will depend upon a variety of factors including the packing of the sample, how finely divided the sample is, and so forth. In this current work, the value of k is assumed to be 1.

In experiments with low evaporation coefficients, this value, α, can be estimated by rearranging eq 7 to

$$P_m = P_{eq} - P_m f\left(\frac{1}{\alpha} + \frac{1}{W_A} - 2\right) \tag{9}$$

Therefore, if a series of effusion experiments are made with cells of different orifice sizes and the data were plotted on a graph as P_m versus $P_m f$ and fit to a straight line, the resulting intercept should yield the equilibrium vapor pressure, P_{eq}, while the value of the evaporation coefficient, α, may be computed from the slope.

A few of additional notes should be made regarding eq 9. First, for orthocylindrical cells, the value of W_A is 0.5, and the quantity $((1/W_A) - 2) = 0$. In this work, the value of W_A is close to 0.5 so the sum of these two terms contribute very little to the sum in the parentheses of eq 9, especially for cases where α is very small. Next, as mentioned earlier the value of k was assumed to be 1. For values of $k > 1$, the value of α will be smaller, and the evaporation coefficients reported in this work are, strictly speaking, $k\alpha$ products, and this should be noted when comparing evaporation coefficient data from other experimental works.

ESTIMATION OF EXPERIMENTAL UNCERTAINTIES

The estimated uncertainties in the current work are similar to those for a previous work with silicon monoxide, and the reader is referred to this work for more detail.[7] As noted in the previous section, values of the equilibrium vapor pressure and evaporation coefficient are taken from plots of P_m versus $P_m f$ at particular temperatures for different effusion orifices. Uncertainties in these quantities arise from the measured temperature, the measured mass loss rate, and cell geometry (cell wall thickness, orifice diameter).

Typical uncertainties for a type-B thermocouple in the experimental temperature range are ± 5 K, and these values are used in this work. As in the case of experimental runs with silicon monoxide, the accuracy of the thermocouple was checked against the melting point of a sample of pure copper with the thermocouple falling within this ± 5 K-band of the copper fusion temperature.[7]

Factors related to cell geometry include the orifice diameter, the depth of the effusion orifice, and the interior cell geometry. The effusion orifice was measured using a microscope and an accurate, moveable stage, and these measurements were estimated to be accurate to within ± 0.02 mm. The wall thickness at the effusion orifice was constant for all the cells used and was measured with a similar uncertainty as (1.27 ± 0.02) mm. To calculate the Clausing factor for the effusion cell used in the Whitmann−Motzfeldt equation, the distance from the top of the evaporating material to the effusion orifice must be known. These interior measurements are not accurately known. Fortunately, the results are not sensitive to these values, especially in the case of very low evaporation coefficients. In this work as well as in previous experiments with silicon monoxide powder, the height from the top of the evaporating material to the effusion orifice was estimated as (10 ± 2) mm, while the evaporating surface area was just taken as the internal cross-sectional area of the inner tube with a diameter of (6.3 ± 0.2) mm.

For an isothermal period, the mean mass loss rates of the 2 min averages described earlier are used as the mass loss rate in eq 2, and the uncertainty in this quantity is estimated as the standard deviation of the measured value. Typically, the predominant source of uncertainty in the calculation of P_m in eq 2 is the mass loss rate. Nevertheless, the uncertainties in all of these measured observables, (temperature, mass loss rate, and cell geometry), on P_m, are considered, and these estimates are added in quadrature as described in the earlier publication for silicon monoxide.[7]

RESULTS

The rate of mass loss from several different effusion cells was monitored over time at several specific temperatures. Afterward, the data from each of these cells at these specific temperatures were plotted in the form given by eq 9. As noted

dx.doi.org/10.1021/je200693d | J. Chem. Eng. Data 2012, 57, 721−728

Table 1. Experimental Data for SiO Vapor Pressure Measurements over a Mixture of Silicon and Silica[a]

T	d	B		m	t	$\dot{m}$		P_m
K	mm	cm^2	W_B	mg	s	$mg \cdot min^{-1}$	f	Pa
1433	1.08	0.00925	0.479	15.34	21000	0.0439 ± 0.0050	0.0140	2.15 ± 0.27
1433	1.24	0.01217	0.510	18.64	21000	0.0532 ± 0.0034	0.0196	1.86 ± 0.15
1433	0.57	0.00257	0.339	6.82	32100	0.013 ± 0.011	0.0027	3.2 ± 2.9
1433	1.72	0.02324	0.583	21.00	21300	0.0592 ± 0.0057	0.0428	0.950 ± 0.096
1443	1.72	0.02324	0.583	21.30	17400	0.07346 ± 0.00058	0.0428	1.183 ± 0.036
1443	0.57	0.00257	0.339	6.30	17100	0.02209 ± 0.00073	0.0027	5.53 ± 0.99
1443	1.08	0.00925	0.479	16.02	17400	0.05522 ± 0.00047	0.0140	2.72 ± 0.16
1443	1.24	0.01217	0.510	17.97	17400	0.06195 ± 0.00069	0.0196	2.18 ± 0.10
1453	0.57	0.00257	0.339	6.33	14700	0.02585 ± 0.00078	0.0027	6.5 ± 1.2
1453	1.72	0.02324	0.583	21.15	14700	0.08636 ± 0.00062	0.0428	1.395 ± 0.043
1453	1.08	0.00925	0.479	15.66	14700	0.0639 ± 0.0011	0.0140	3.16 ± 0.19
1453	1.24	0.01217	0.510	17.36	14700	0.07084 ± 0.00069	0.0196	2.50 ± 0.12
1462	1.72	0.02324	0.583	21.31	12600	0.10152 ± 0.00061	0.0428	1.645 ± 0.050
1462	1.24	0.01217	0.510	17.33	12600	0.08253 ± 0.00069	0.0196	2.92 ± 0.14
1462	1.08	0.00925	0.479	15.71	12600	0.0749 ± 0.0020	0.0140	3.71 ± 0.23
1462	0.57	0.00257	0.339	6.28	12300	0.0307 ± 0.0011	0.0027	7.7 ± 1.4
1472	1.08	0.00925	0.479	15.64	10500	0.0893 ± 0.0035	0.0140	4.44 ± 0.31
1472	1.24	0.01217	0.510	16.73	10500	0.09560 ± 0.00079	0.0196	3.39 ± 0.16
1472	1.72	0.02324	0.583	20.91	10500	0.11949 ± 0.00069	0.0428	1.943 ± 0.059
1472	0.57	0.00257	0.339	6.57	10500	0.0376 ± 0.0012	0.0027	9.5 ± 1.7
1481	0.57	0.00257	0.339	6.77	9000	0.0452 ± 0.0079	0.0027	11.5 ± 2.8
1481	1.72	0.02324	0.583	21.09	9000	0.14060 ± 0.00072	0.0428	2.293 ± 0.069
1481	1.08	0.00925	0.479	15.58	9000	0.10391 ± 0.00093	0.0140	5.19 ± 0.30
1481	1.24	0.01217	0.510	16.96	9000	0.11307 ± 0.00095	0.0196	4.02 ± 0.19
1491	1.08	0.00925	0.479	15.53	7500	0.1242 ± 0.0012	0.0140	6.22 ± 0.36
1491	1.24	0.01217	0.510	16.77	7500	0.1341 ± 0.0012	0.0196	4.79 ± 0.23
1491	1.72	0.02324	0.583	21.40	7800	0.16467 ± 0.00091	0.0428	2.694 ± 0.081
1491	0.57	0.00257	0.339	7.38	7500	0.0590 ± 0.0014	0.0027	15.0 ± 2.7
1500	1.08	0.00925	0.479	15.54	6300	0.14790 ± 0.00079	0.0140	7.43 ± 0.42
1500	1.24	0.01217	0.510	16.48	6300	0.1569 ± 0.0010	0.0196	5.62 ± 0.26
1500	1.72	0.02324	0.583	21.12	6600	0.1921 ± 0.0013	0.0428	3.154 ± 0.096
1500	0.57	0.00257	0.339	6.95	6300	0.0661 ± 0.0016	0.0027	16.9 ± 3.0
1510	1.72	0.02324	0.583	20.04	5400	0.2225 ± 0.0016	0.0428	3.66 ± 0.11
1510	1.08	0.00925	0.479	15.44	5400	0.1717 ± 0.0013	0.0140	8.65 ± 0.50
1510	1.24	0.01217	0.510	16.56	5400	0.18399 ± 0.00093	0.0196	6.61 ± 0.31
1510	0.57	0.00257	0.339	7.01	5400	0.07790 ± 0.00090	0.0027	19.9 ± 3.5
1519	1.24	0.01217	0.510	16.10	4500	0.2146 ± 0.0011	0.0196	7.74 ± 0.36
1519	0.57	0.00257	0.339	7.16	4800	0.0893 ± 0.0017	0.0027	22.9 ± 4.1
1519	1.08	0.00925	0.479	14.96	4500	0.19950 ± 0.00098	0.0140	10.08 ± 0.58
1520	1.72	0.02324	0.583	20.52	4800	0.2567 ± 0.0018	0.0428	4.24 ± 0.13
1530	1.72	0.02324	0.583	19.63	3900	0.3018 ± 0.0017	0.0428	5.00 ± 0.15
1530	1.08	0.00925	0.479	15.36	3900	0.2363 ± 0.0011	0.0140	11.98 ± 0.68
1530	1.24	0.01217	0.510	16.53	3900	0.2543 ± 0.0014	0.0196	9.20 ± 0.43
1530	0.57	0.00257	0.339	6.79	3900	0.1043 ± 0.0016	0.0027	26.9 ± 4.7
1540	0.57	0.00257	0.339	6.35	3300	0.1151 ± 0.0020	0.0027	29.8 ± 5.3
1540	1.72	0.02324	0.583	19.02	3300	0.3457 ± 0.0022	0.0428	5.75 ± 0.17
1540	1.08	0.00925	0.479	14.99	3300	0.2725 ± 0.0019	0.0140	13.86 ± 0.79
1540	1.24	0.01217	0.510	16.21	3300	0.2946 ± 0.0020	0.0196	10.69 ± 0.50
1549	0.57	0.00257	0.339	6.32	2700	0.1398 ± 0.0046	0.0027	36.3 ± 6.5
1549	1.72	0.02324	0.583	17.89	2700	0.3972 ± 0.0023	0.0428	6.63 ± 0.20
1549	1.08	0.00925	0.479	14.08	2700	0.3127 ± 0.0021	0.0140	15.96 ± 0.91
1549	1.24	0.01217	0.510	15.28	2700	0.3397 ± 0.0023	0.0196	12.37 ± 0.58
1560	0.57	0.00257	0.339	4.64	1800	0.1540 ± 0.0032	0.0027	40.1 ± 7.1
1560	1.08	0.00925	0.479	12.78	2100	0.3648 ± 0.0026	0.0140	18.7 ± 1.1
1560	1.24	0.01217	0.510	13.95	2100	0.3977 ± 0.0036	0.0196	14.53 ± 0.68
1560	1.72	0.02324	0.583	18.48	2400	0.4623 ± 0.0040	0.0428	7.74 ± 0.24
1570	1.72	0.02324	0.583	18.41	2100	0.5256 ± 0.0049	0.0428	8.83 ± 0.27
1570	1.08	0.00925	0.479	14.57	2100	0.4159 ± 0.0028	0.0140	21.4 ± 1.2
1570	1.24	0.01217	0.510	16.00	2100	0.4567 ± 0.0061	0.0196	16.74 ± 0.81

dx.doi.org/10.1021/je200693d | J. Chem. Eng. Data 2012, 57, 721−728

Table 1. continued

T	d	B		m	t	$\dot{m}$		P_m
K	mm	cm^2	W_B	mg	s	$mg \cdot min^{-1}$	f	Pa
1579	1.08	0.00925	0.479	14.18	1800	0.4726 ± 0.0030	0.0140	24.3 ± 1.4
1579	1.24	0.01217	0.510	15.62	1800	0.5213 ± 0.0060	0.0196	19.16 ± 0.91
1579	1.72	0.02324	0.583	14.83	1500	0.5927 ± 0.0041	0.0428	9.98 ± 0.30
1589	1.08	0.00925	0.479	10.72	1200	0.5353 ± 0.0042	0.0140	27.7 ± 1.6
1589	1.24	0.01217	0.510	11.91	1200	0.5944 ± 0.0086	0.0196	21.9 ± 1.1
1589	1.72	0.02324	0.583	16.80	1500	0.6729 ± 0.0077	0.0428	11.37 ± 0.36
1598	1.72	0.02324	0.583	18.94	1500	0.7555 ± 0.0091	0.0428	12.80 ± 0.41
1598	1.08	0.00925	0.479	15.16	1500	0.6048 ± 0.0094	0.0140	31.3 ± 1.8
1598	1.24	0.01217	0.510	16.89	1500	0.6743 ± 0.0080	0.0196	24.9 ± 1.2
1608	1.72	0.02324	0.583	16.83	1200	0.837 ± 0.013	0.0428	14.23 ± 0.48
1608	1.08	0.00925	0.479	13.52	1200	0.673 ± 0.011	0.0140	35.0 ± 2.1
1608	1.24	0.01217	0.510	15.13	1200	0.7544 ± 0.0098	0.0196	28.0 ± 1.3

[a]Listed in the table are the run temperature, T/K, the diameter of the cell orifice, d/mm, the area of the effusion orifice, B/cm^2, the Clausing factor for the orifice, W_B, the total mass lost during the isothermal period, m/mg, the duration of the isothermal period, t/s, the computed loss rate and its estimated uncertainty, $\dot{m}/(mg \cdot min^{-1})$, the factor, f, as given by eq 8 for each cell, and the value of the apparent, measured vapor pressure, P_m/Pa, as given by eq 2 for each run. The area of the evaporating surface, A, for all cells was taken as the internal cross-sectional area of the cell (0.317 cm^2), and the Clausing factor for all the cells, W_A, was 0.412.

earlier, a linear fit to this form should give the equilibrium vapor pressure as the intercept and the evaporation coefficient may be computed from the slope. The raw data from each of the experimental runs are given in Table 1. These observables include the cell temperature, orifice diameter and mass loss rate given in columns 1, 2, and 7, respectively. Quantities related to the cell geometry are also given in the table. These include B, the effusion area (column 3), W_B, the Clausing factor for the effusion orifice (column 4), and the f parameter for the cell (column 8) as defined in eq 8 with the assumption that the effective evaporation area is given by the internal cross-sectional area of the sample cell. As described in the earlier section, the mass loss rate, $\dot{m}$, and its associated uncertainty are calculated from the averaging procedure noted earlier. In addition, the length of the isothermal periods and the total mass lost during the time are given in columns 6 and 5, respectively, of Table 1. Although, the mass loss rates calculated from these starting and ending values should be extremely close to the values reported in column 7 of the table, there may be slight differences between the two. Several different cells were used in these experiments with orifice diameters ranging from (0.57 to 2.19) mm. The values of the measured vapor pressures, P_m, and their uncertainty estimates are given in column 9 of the table.

The uncertainty in these values of P_m varies based mainly on the uncertainty in the mass loss measurement. When constructing the Whitmann−Motzfeldt plot of P_m versus $P_m f$ for the different cells, this results in a varying uncertainty in both the x and y coordinates of the graph. Therefore, a computer routine, FITEXY, was used that is capable of fitting a line through data when there is uncertainty in both coordinates.[24] Weighting factors were constructed from the uncertainty, σ_i, in each coordinate and given by w_i where

$$w_i = 1/\sigma_i^2 \tag{10}$$

The code for this FITEXY subroutine was taken directly from ref 24. Another advantage of using this routine is that it provides uncertainty estimates for both the slope and interecept, and these were used to compute the estimated uncertainties in the final quantities. Plots of each isotherm were made, and the weighted fits were compared to unweighted fits to verify that the final data were not incorrectly influenced by the weighting factors. In approximately half of the data points, the unweighted and weighted results were essentially identical, and in the remaining fraction, the results were only modestly different.

These derived values are given in Table 2. In constructing the Whitmann−Motzfeldt plots, the data from Table 1 reduces down to the 19 points given in Table 2. A minimum of three points were used for each of the final values given in this table. Shown in the table are the isothermal temperature, the evaporation coefficient, and the equilibrium vapor pressure. A plot of the evaporation coefficient values and their associated uncertainty is given in Figure 2. These values range from approximately 0.005 to 0.009, and there appears to be a slight

Table 2. Evaporation Coefficient, α, Equilibrium Vapor Pressure, P_{eq}/Pa, and Enthalpy of Reaction, $\Delta_{rxn}H°(298.15\ K)/(kJ \cdot mol^{-1})$, for SiO Derived from the Measurements Using Three Different Knudsen Cell Orifice Sizes

T		P_{eq}	$\Delta_{rxn}H°(298.15\ K)$
K	α	Pa	$kJ \cdot mol^{-1}$
1433	0.0089 ± 0.0040	5.7 ± 2.2	363.8 ± 4.7
1443	0.0082 ± 0.0020	7.4 ± 1.4	363.0 ± 2.3
1453	0.0086 ± 0.0021	8.3 ± 1.6	363.9 ± 2.3
1462	0.0086 ± 0.0021	9.8 ± 1.9	364.2 ± 2.4
1472	0.0082 ± 0.0021	12.0 ± 2.5	364.0 ± 2.6
1481	0.0085 ± 0.0025	13.7 ± 3.2	364.5 ± 2.9
1491	0.0069 ± 0.0020	19.1 ± 4.6	362.7 ± 3.0
1500	0.0070 ± 0.0019	22.3 ± 5.1	362.9 ± 2.9
1510	0.0068 ± 0.0019	26.6 ± 6.1	362.9 ± 2.9
1520	0.0067 ± 0.0018	31.2 ± 7.1	363.0 ± 2.9
1530	0.0066 ± 0.0018	37.2 ± 8.4	363.2 ± 2.9
1540	0.0068 ± 0.0018	42.1 ± 9.0	363.7 ± 2.8
1549	0.0064 ± 0.0017	51 ± 12	363.3 ± 3.0
1560	0.0067 ± 0.0017	57 ± 12	364.2 ± 2.8
1570	0.0063 ± 0.0028	69 ± 31	363.8 ± 6.2
1579	0.0059 ± 0.0027	82 ± 39	363.5 ± 6.8
1589	0.0059 ± 0.0027	94 ± 46	363.9 ± 7.0
1598	0.0056 ± 0.0027	111 ± 59	363.6 ± 7.9
1608	0.0054 ± 0.0027	128 ± 74	363.7 ± 8.8

dx.doi.org/10.1021/je200693d | J. Chem. Eng. Data 2012, 57, 721−728

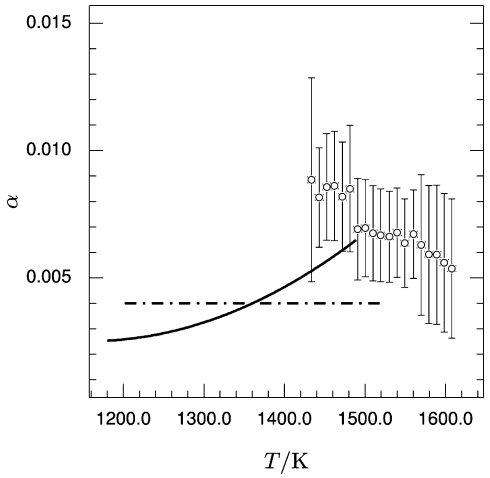

Figure 2. Evaporation coefficient, α, for a mixture of silicon and silica. Shown in the figure are experimental data from this work, ○, and values reported by Rocabois et al., —, and Gunther, –·–.

decrease in these values with temperature. On the basis of the relatively large uncertainty in these values, it would likely be hazardous to ascribe any significance to this trend. For this reason, it is more reasonable to report a single value of (0.007 ± 0.002) for this temperature range.

In 1958, Gunther estimated the evaporation coefficient for the silicon/silica reaction to be approximately $4{\cdot}10^{-3}$, and this value is shown in the graph as the dashed–dotted line over the experimental temperature range reported by Gunther.[25] The values reported in this work are of the same, low order of magnitude as those of Gunther but are slightly higher. In 1992, Rocabois et al. studied both the evaporation coefficient and the equilibrium vapor pressure over amorphous silicon monoxide and mixtures of silicon and silica.[16] One focus of this work was to study the stability of nominally amorphous silicon monoxide. Rather than being a stable compound, research suggested that silicon monoxide exists as an intimate mixture of silicon and silica over very small domains. Data were taken by these authors using multiple Knudsen cells and mass spectrometry.

Measured evaporation coefficients for the silicon/silica mixture were much smaller than those for the amorphous silicon monoxide. For vitreous silica, these values reportedly ranged from $2{\cdot}10^{-4}$ to $8{\cdot}10^{-3}$ over the temperature range (1097 to 1489) K, while those for amorphous silicon monoxide were approximately an order of magnitude higher.[16] In addition to vitreous silica, Rocabois et al. also studied the evaporation coefficients for the reaction of silicon with cristobalite, finding even lower values of the evaporation coefficient for this reaction. In this case, they reported a constant evaporation coefficient of $(1.1 \pm 0.5){\cdot}10^{-3}$ over the temperature range (1172 to 1404) K. Rocabois et al. provided a fit to their evaporation coefficient data for their vitreous silica and silicon data, and this fit is shown as the solid line in Figure 2. There is some overlap between the data range covered by Rocabois et al. and the results presented in this work, and there seems to be reasonable agreement between the magnitude of the evaporation coefficient in this range, although the two sets of data seem to follow very different temperature trends.

A plot of the equilibrium vapor pressure values from Table 2 is given in Figure 3 by the open circles. A fit to the equilibrium vapor pressure values is given by

$$\log_{10}(P/\mathrm{Pa}) = (13.25 \pm 0.89) - \frac{(17900 \pm 1300)}{T/\mathrm{K}} \qquad (11)$$

over the temperature range (1433 to 1608) K and is shown as the solid line in Figure 3. This fit was weighted based on similar weighting factors as given in eq 10, but only for the y-values since the estimated uncertainty in the temperatures are equal. Due to the low evaporation coefficients of the silicon–silica

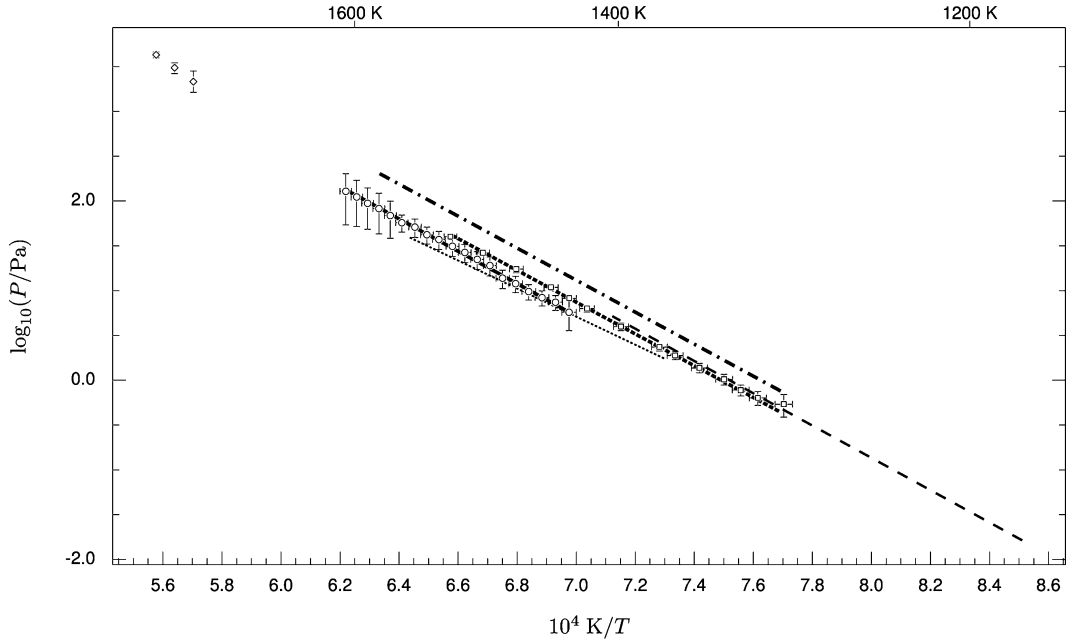

Figure 3. Comparison of silicon monoxide vapor pressure data over a mixture of silicon and silica. Shown in the figure are experimental data reported in this work, ○, and a linear fit to these data, —, a fit to experimental data from Rocabois et al., – –, a fit to experimental data taken by Kubaschewski and Chart, –·–, experimental data points from Huang et al., ◊, and a fit to data taken by Shornikov and Archakov, ···. Also shown for comparison is experimental data for silicon monoxide evaporation, □, reported in a previous study and a fit to these data, ---.

dx.doi.org/10.1021/je200693d | J. Chem. Eng. Data 2012, 57, 721–728

mixture, the uncertainties in these fit parameters are more than twice as large as the uncertainties in the fit for silicon monoxide vapor pressure over silicon monoxide powder.[7] Although there is considerable uncertainty in the equilibrium vapor pressure values, the linear fit to the data is very good.

The equilibrium vapor pressures have also been used to calculate the third law enthalpy of reaction values, and these are given in column 4 of Table 2. In computing these values, thermodynamic data for silicon and silicon dioxide were taken from the National Institute of Standards and Technology/Joint Army, Navy, Air Force (NIST-JANAF) tables.[26] It should also be noted that these heat capacity data used to generate the free energy functions for the third law analysis are identical to the values used in the study of nominal $SiO_{(am)}$ evaporation. In addition, it is assumed that the uncertainty in these enthalpy values arises entirely from the uncertainty in the vapor pressure data. These values range from (363 to 365) kJ·mol^{-1} and do not seem to follow any temperature trend. Therefore, for this work the third law enthalpy of reaction at 298.15 K, $\Delta_{rxn}H°(298.15\ K)$, is taken as (363.6 ± 4.1) kJ·mol^{-1}. Using eq 11, the enthalpy of the reaction at a mean experimental temperature of 1521 K is (343 ± 25) kJ·mol^{-1}. Again, using the heat capacity data for silicon and silicon monoxide as noted above, this gives the second law enthalpy of reaction at 298.15 K for the data as (355 ± 25) kJ·mol^{-1}. There is considerable uncertainty in this second law value due to the large uncertainty in the slope of eq 11. These values are in fair agreement and certainly agree within the experimental uncertainty reported for each value.

A comparison with some of the most recent measurements of SiO vapor pressure is also given in Figure 3. In 1974, Kubaschewski and Chart measured the vapor pressure of SiO over a mixture of silicon and silica using a thermogravimetric and the Knudsen effusion method.[27] Data were taken in the temperature range of (1270 to 1600) K, using different orifice diameters and extracting estimates of the evaporation coefficient and equilibrium vapor pressures in the same manner used in this work. These authors fit their vapor pressure data to the following equation:

$$\log_{10}(P/\mathrm{Pa}) = 13.613 - \frac{17850}{T/\mathrm{K}} \qquad (12)$$

and this fit is shown by the dashed−dotted line in Figure 3. The slope of this fit and the current data from this work are very close, but the magnitude of the Kubashewski and Chart vapor pressures are larger than in this work. Evaporation coefficients were not specifically reported in the work of Kubaschewski and Chart but can be extracted from their vapor pressure data. Shornikov and Archakov calculated the evaporation coefficient for the silicon + cristobalite mixture as $(1.43 \pm 0.16)\cdot10^{-3}$ from Kubaschewski and Chart's vapor pressure measurements.[28]

As previously mentioned, Rocabois et al. studied both the evaporation coefficients of silicon monoxide gas over silicon monoxide powder and mixtures of silicon/silica in 1992. Although they found large differences in the evaporation coefficients for both of these systems, the vapor pressures in both cases were essentially identical within the experimental uncertainty in their work. Individual vapor pressure values were not reported in their work, only graphs of fits to their data. The fit to their SiO vapor pressure data is shown as the long dashed line in Figure 3. In a previous study with silicon monoxide, very close agreement was found between the measured vapor pressures and data from Rocabois et al. with an overlap in the experimental temperature range. These data for the evaporation of silicon monoxide powder are shown as the square data points and a fit to these points (short dashed line) in Figure 3. For the current data for silicon and silica evaporation, the vapor pressures fall somewhat below these data for silicon monoxide powder, and agreement between the two is just at the edge of the estimated uncertainty between the two measurements.

Later in 2000, Shornikov and Archakov published results from a study of the evaporation of silicon monoxide, focusing on the determination of the evaporation coefficients for amorphous silicon monoxide and mixtures of silicon and silica.[28] Similar to Rocabois et al., these authors also used the Knudsen effusion combined with mass spectrometry. For a mixture of cristobalite and silicon, Shornikov and Archakov found the evaporation coefficient to be $(1.65 \pm 0.10)\cdot10^{-3}$, a value which compares very favorably with results from Kubaschewski and Chart $(1.43 \pm 0.16)\cdot10^{-3}$ and Rocabois et al. $(1.1 \pm 0.5)\cdot10^{-3}$.[28]

Although the equilibrium vapor pressures for silicon monoxide were not reported by Shornikov and Archakov, they can be estimated using data presented by the authors in graphs of P_m and reported f parameters for their cells. These data were digitized for the four cells used to study the evpaoration coefficients of the crystalline silica and silicon system. In constructing the Whitmann−Motzfeldt plot, the cell with the largest orifice diameter did not seem consistent with the remaining data so only the three cells with the smallest effusion orifices were used to estimate the equilibrium vapor pressure. This estimate of the vapor pressure from Shornikov and Archakov is given as the dotted line in Figure 3. These extrapolated, equilibrium vapor pressure values are approximately 20 % higher than the experimentally measured vapor pressures taken with the cell with the smallest effusion orifice. These values certainly lie within the experimental uncertainty of this work, yet have a slightly different slope.

Huang et al. studied the vapor pressure over a silicon and silica mixture at pressures much higher than those available via Knudsen effusion.[29] The goal of this work was to estimate the equilibrium vapor pressure of SiO over this system to aid in modeling the evaporation rate of SiO in the Cz−Si system. These authors built an ampule of silica, placed an amount of silicon within the ampule, and then evacuated and sealed the ampule. The ampule was then placed under a carbon heater within a vacuum chamber charged with an atmosphere of argon gas. As the ampule was heated, the silicon and silica would exert a vapor pressure that would distort the ampule. The outside argon pressure was then adjusted to eliminate the distortion of the cell, thus matching the SiO vapor pressure within the cell. These authors measured SiO vapor pressure at three temperatures with estimated uncertainties in these values of ± 130 Pa, and these values are shown in Figure 3 as the three points at the highest temperatures of the plot. Since the cell of Huang et al. was sealed, the pressure exerted on the walls of their ampule would equal the equilibrium vapor pressure of silicon monoxide over a mixture of silicon and silica, and the evaporation coefficients do not play a role in this system.

It is interesting to note that there is reasonably good agreement on the equilibrium vapor pressure of silicon monoxide between the collections of data when the evaporation coefficient is correctly applied. For example, there is reasonable agreement with the vapor pressure data over amorphous silicon monoxide powder in spite of the fact that the evaporation coefficient for this system is approximately an order of

magnitude higher than for the silicon/silica system. Even in the case where there are different forms of silica used (vitreous versus crystalline), the equilibrium vapor pressures for the silicon monoxide gas are approximately equal when the evaporation coefficient is correctly taken into account.

CONCLUSION

The evaporation coefficients and equilibrium vapor pressure of silicon monoxide gas over a mixture of silicon and vitreous silica has been studied using Knudsen effusion. The rate of mass loss of silicon monoxide gas was measured using a thermogravimetric balance. Due to the very low evaporation coefficient for this system, several experiments with Knudsen cells of different effusion orifice sizes were made, and the data taken at constant temperatures were plotted and extrapolated to zero orifice size to get equilibrium vapor pressures. Vapor pressure and evaporation coefficient data were measured over the temperature range of (1433 to 1608) K. The resulting evaporation coefficient, (0.007 ± 0.002), was very low and in reasonable agreement with measurements by other research groups. The enthalpy of reaction at 298.15 K for this reaction was calculated via second and third law analyses as (355 ± 25) kJ·mol^{-1} and (363.6 ± 4.1) kJ·mol^{-1}, respectively, and was in agreement within the uncertainty in the values. It is thought that amorphous silicon monoxide is not a true compound, but rather an intimate mixture of silicon and silicon monoxide. Therefore, the kinetics of the evaporation reaction will depend upon the value of the evaporation coefficient, but the equilibrium vapor pressure for the (nominally) amorphous silicon monoxide system and an ordinary mixture of silicon and silica should be identical. A comparison of the data for the current silicon and silica reaction with a previous experimental work with silicon monoxide powder shows that this is the case and provides further evidence that solid silicon monoxide is an intimate mixture of small domains of silicon and silica rather than a true compound.

AUTHOR INFORMATION

Corresponding Author

*E-mail: frank.ferguson@nasa.gov.

REFERENCES

(1) Li, Y.; Li, M.; Imaishi, N.; Akiyama, Y.; Tsukada, T. Oxygen-transport phenomena in a small silicon Czochralski furnace. *J. Cryst. Growth* **2004**, *267*, 466−474.

(2) Schnurre, S. M.; Schmid-Fetzer, R. Reactions at the liquid silicon silica glass interface. *J. Cryst. Growth* **2003**, *250*, 370−381.

(3) Schnurre, S. M.; Gröbner, J.; Schmid-Fetzer, R. Thermodynamics and phase stability in the Si-O system. *J. Non-Cryst. Solids* **2004**, *336*, 1−24.

(4) Jana, S.; Dost, S.; Kumar, V.; Durst, F. A numerical simulation study for the Czochralski growth process of Si under magnetic field. *Int. J. Eng. Sci.* **2006**, *44*, 554−573.

(5) Su, W.; Zua, R.; Mazaev, K.; Kalaev, V. Optimization of crystal growth by changes of flow guide, radiation shield and sidewall insulation in Cz Si furnace. *J. Cryst. Growth* **2010**, *312*, 495−501.

(6) Jeong, K. S.; Winters, J. M.; Le Bertre, T.; Sedlmayr, E. Self-consistent modeling of the outflow from the O-rich Mira IRC-20197. *Astron. Astrophys.* **2003**, *407*, 191−206.

(7) Ferguson, F. T.; Nuth, J. A. III. Vapor Pressure of Silicon Monoxide. *J. Chem. Eng. Data* **2008**, *53*, 2824−2832.

(8) Nuth, J. A.; Donn, B. Experimental Studies of the Vapor Phase Nucleation of Refractory Compounds. I. The condensation of SiO. *J. Chem. Phys.* **1982**, *77*, 2639−2646.

(9) Schick, H. L. A Thermodynamic Analysis of the High-Temperature Vaporization Properties of Silica. *Chem. Rev.* **1960**, *60*, 331−362.

(10) Nuth, J. A.; Ferguson, F. T. Silicates do nucleate in oxygen-rich circumstellar outflows: new vapor pressure data for SiO. *Astrophys. J.* **2006**, *649*, 1178−1183.

(11) Brewer, L.; Edwards, R. K. The Stability of SiO Solid and Gas. *J. Phys. Chem.* **1954**, *58*, 351−358.

(12) Porter, R. F.; Chupka, W. A.; Inghram, M. G. Mass Spectrometric Study of Gaseous Species in the Si-SiO_2 System. *J. Chem. Phys.* **1955**, *23*, 216−217.

(13) Friede, B.; Jansen, M. Some comments on so-called "silicon monoxide". *J. Non-Cryst. Solids* **1996**, *204*, 202−203.

(14) Schulmeister, K.; Mader, W. TEM investigation on the structure of amorphous silicon monoxide. *J. Non-Cryst. Solids* **2003**, *320*, 143−150.

(15) Hohl, A.; Wider, T.; van Aken, P. A.; Weirich, T. E.; Genninger, G.; Vidal, M.; Oswald, S.; Deneke, C.; Mayer, J.; Fuess, H. An interface clusters mixture model for the structure of amorphous silicon monoxide (SiO). *J. Non-Cryst. Solids* **2003**, *320*, 255−280.

(16) Rocabois, P.; Chatillon, C.; Bernard, C. Vapor pressure and evaporation coefficient of SiO (amorphous) and $SiO_{2(S)}$ + $Si_{(S)}$ mixtures by the multiple Knudsen cell mass spectrometric method. *Rev. Int. Hautes Temp. Refract.* **1992**, *28*, 37−48.

(17) Ferguson, F. T.; Gardner, K. G.; Nuth, J. A. III. The Vapor Pressure of Palladium from 1473 to 1973 K. *J. Chem. Eng. Data* **2006**, *51*, 1509−1515.

(18) Clausing, P. The Flow of Highly Rarefied Gases through Tubes of Arbitrary Length. *Vac. Sci. Technol.* **1971**, *8*, 636−756.

(19) Berman, A. S. Free Molecule Transmission Probabilities. *J. Appl. Phys.* **1965**, *10*, 3356.

(20) Szwemin, P.; Niewiński, M. Comparison of transmission probabilities calculated by Monte Carlo simulation and analytical methods. *Vacuum* **2002**, *67*, 359−362.

(21) Drowart, J.; Chatillon, C.; Hastie, J.; Bonnell, D. High-Temperature Mass Spectrometry: Instrumental Techniques, Ionization Cross-sections, Pressure Measurements, and Thermodynamic Data. *Pure Appl. Chem.* **2005**, *77*, 693−737.

(22) Whitman, C. On the Measurement of Vapor Pressures by Effusion. *J. Chem. Phys.* **1952**, *20*, 161−164.

(23) Motzfeldt, K. The Thermal Decomposition of Sodium Carbonate by the Effusion Method. *J. Phys. Chem.* **1955**, *59*, 139−147.

(24) Press, W. H.; Teukolsky, S. A.; Vetterling, W. T.; Flannery, B. P. *Numerical Recipes in C*; Cambridge University Press: Cambridge, 1992.

(25) Gunther, K. G. On the measurement of the vapor pressure and evaporation rate of glass-forming substances. *Glastech. Ber.* **1958**, *31*, 9−15.

(26) Chase, M. W., Jr. *NIST-JANAF thermochemical tables*; American Institute of Physics: New York, 1998.

(27) Kubaschewski, O.; Chart, T. G. Silicon monoxide pressures due to the reaction between solid silicon and silica. *J. Chem. Thermodyn.* **1974**, *6*, 467−476.

(28) Shornikov, S. I.; Archakov, I. Y. *High Temperature Study of the Evaporation of Silicon Monoxide High Temperature Materials Chemistry*, Proceedings of the 10th International IUPAC Conference 2000; pp 431−434.

(29) Huang, X.; Terashima, K.; Hoshikawa, K. SiO Vapor Pressure in an SiO_2 Glass/Si Melt/SiO Gas Equilibrium System. *Jpn. J. Appl. Phys.* **1999**, *38*, L1143−L1155.